Environmental Science & Technology

Article

pubs.acs.org/est

Autonomous Marine Robotic Technology Reveals an Expansive Benthic Bacterial Community Relevant to Regional Nitrogen Biogeochemistry

David L. Valentine,[*,†,‡] G. Burch Fisher,[†,¶] Oscar Pizarro,[§] Carl L. Kaiser,[∥] Dana Yoerger,[∥] John A. Breier,[∥,▽] and Jonathan Tarn[⊥]

[†]Department of Earth Science and [‡]Marine Science Institute, University of California, Santa Barbara, California 93106, United States

[¶]Jackson School of Geosciences, University of Texas, Austin, Texas 78712, United States

[§]Australian Center for Field Robotics, University of Sydney, Sydney, Australia

[∥]Department of Applied Ocean Physics and Engineering, Woods Hole Oceanographic Institution, Woods Hole, Massachusetts 02543, United States

[⊥]Interdepartmental Graduate Program in Marine Science, University of California, Santa Barbara, California 93106, United States

Supporting Information

ABSTRACT: Benthic accumulations of filamentous, mat-forming bacteria occur throughout the oceans where bisulfide mingles with oxygen or nitrate, providing key but poorly quantified linkages between elemental cycles of carbon, nitrogen and sulfur. Here we used the autonomous underwater vehicle *Sentry* to conduct a contiguous, 12.5 km photoimaging survey of sea-floor colonies of filamentous bacteria between 80 and 579 m water depth, spanning the continental shelf to the deep suboxic waters of the Santa Barbara Basin (SBB). The survey provided >31 000 images and revealed contiguous, white-colored bacterial colonization coating > ∼80% of the ocean floor and spanning over 1.6 km, between 487 and 523 m water depth. Based on their localization within the stratified waters of the SBB we hypothesize a dynamic and annular biogeochemical zonation by which the bacteria capitalize on periodic flushing events to accumulate and utilize nitrate. Oceanographic time series data bracket the imaging survey and indicate rapid and contemporaneous nitrate loss, while autonomous capture of microbial communities from the benthic boundary layer concurrent with imaging provides possible identities for the responsible bacteria. Based on these observations we explore the ecological context of such mats and their possible importance in the nitrogen cycle of the SBB.

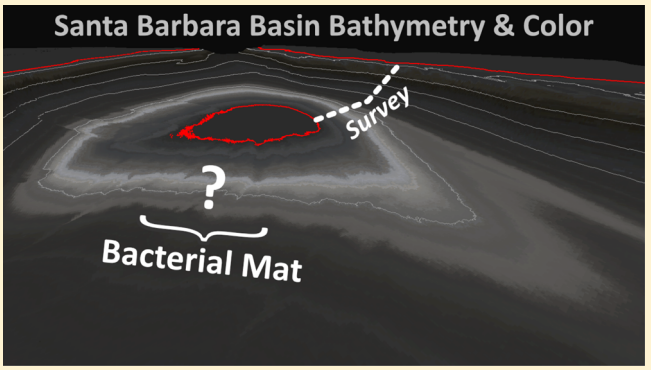

INTRODUCTION

Oceanic waters face oxygen depletion when aerobic respiration exceeds the capacity for reoxygenation by mixing, photosynthesis and atmospheric exchange. Important to ocean biogeochemistry and ecology, this situation occurs both by human influence, for example, so-called dead zones, and through natural processes, for example, oxygen minimum zones (OMZs).[1,2] When faced with oxygen limitation marine microbiota first turn to nitrate as an alternative electron acceptor, oxidizing organic and inorganic substrates with concurrent reduction of nitrate to nitrite, ammonium, nitrous oxide or dinitrogen.[3,4] Denitrification refers to the loss of bioavailable nitrogen from the ecosystem through the subset of these processes for which the nitrogenous products are in gaseous form,[5] for example, nitrous oxide or dinitrogen; denitrification is prevalent in areas where oxygen concentration is kept below ∼5 μM, and serves as the primary global sink of bioavailable nitrogen. Nitrate reduction and denitrification are also key drivers of carbon remineralization in the ocean,[6] being prevalent in areas of high productivity or restricted circulation,[6−8] notably along continental margins where an oceanic OMZ intersects high rates of sedimentation.[9,10] The silled Santa Barbara Basin is an example of such an area[11] and previous studies using stable isotopes at this location demonstrate that at least 75% of nitrate utilization occurs within the sediment.[12]

While many bacterial groups are capable of denitrification, marine sediments can host abundant communities of filamentous, mat-forming bacteria, for example, *Beggiatoa*,

Received: July 17, 2016
Revised: September 15, 2016
Accepted: September 22, 2016

DOI: 10.1021/acs.est.6b03584
Environ. Sci. Technol. XXXX, XXX, XXX−XXX

Thioploca, and *Thiothrix*,[13] that are capable of reducing nitrate to nitrite or ammonium but not necessarily to molecular nitrogen or nitrous oxide.[14] These mat-forming communities can host a rich assortment of bacterial phyla that collectively couple oxygen or nitrate reduction to sulfide oxidation.[15] Large filamentous bacteria can also physically host anaerobic, ammonium-oxidizing (annamox) bacteria[16,17] that complete the denitrification process through coupling of nitrite and ammonium. Due to commonalities such as a filamentous appearance, gliding motility, chemotrophic metabolism, and accumulation of elemental sulfur granules, as well as uncertainties with respect to the range of physiological capabilities exhibited by each genus,[18] filamentous sulfur bacteria are often considered as a collective. However, other aspects of physiology distinguish these groups, notably, the ability of some strains to hyperaccumulate nitrate in storage vacuoles—to concentration of at-least 500 mM,[15] distinctive specificity for oxygen, and distinctive modes of chemotaxis.[14] These physiologies enable sulfide-oxidizing bacterial mats to poise themselves along stable redox gradients, to capitalize on fluctuating environmental redox conditions, or to migrate between disconnected substrate supplies.[19]

The SBB is known to host mats of nitrate accumulating, filamentous sulfur bacteria near its depocenter[20−22] where sediment becomes rapidly sulfidic.[23−25] However, the mats' spatial extent, temporal persistence, and contribution to sediment nitrate utilization[12] are not established. In this work, we set out to use autonomous underwater vehicle (AUV) technology to document changes in benthic communities along the strong redox gradient that forms during periods of stratification in the SBB. In doing so, we identified unexpected depth zonation of bacterial mat at the sea floor that is suggestive of an important and dynamic role modulating nitrogen biogeochemistry in this environment. The present report focuses on the distribution of microbial communities in the SBB including the benthic mats and the overlying benthic boundary layer. These observations are placed in a dynamic context using oceanographic time-series data to explore broader implications for the biogeochemistry of the SBB and the ecology of the microbial community.

EXPERIMENTAL SECTION

The AUV *Sentry* was used for these studies. *Sentry* is a custom built AUV, owned and operated by the National Deep Submergence Facility at Woods Hole Oceanographic Institution,[26] made available for this study through the University National Oceanographic Laboratory System. Mission programming for Dive 204 was conducted immediately preceding launch on 7 October 2013 and involved four primary components. First was a 12.5 km transit from the deep SBB to the continental shelf at an altitude of 3.5 m and a velocity of 0.38 m s^{-1}. Second was a concurrent photo survey, involving the Serpent stereo camera system, consisting of two AVT Prosilica GC1380 (one monochrome, one color) triggered simultaneously. The cameras have a field of view of 42° × 34° and baseline of approximately 90 mm. The imagery was acquired at 1 Hz, with two triggered LED pucks providing illumination. At the target altitude and speed the imagery had approximately 82% overlap. Third was the collection of particulate matter and pelagic bacteria at different locations along the transit, using a custom in situ pump and filtration system, the SUPR sampler.[27] Fourth, was a 12.2 km transit from the continental shelf to the deep SBB at an altitude of 30 m and a velocity of 0.71 ms^{-1}, for purposes of conducting a high-resolution multibeam survey of the imaged terrain. The duration of the survey was 13.5 h.

Depth distributions of physical properties and chemical concentrations were provided by the California Cooperative Oceanic Fisheries Investigations (CalCOFI) for a single station in the SBB, occupied on three occasions: 16 April 2013; 16 July 2013; and 24 November 2013. The data was downloaded from http://www.calcofi.org/data.html and included concentration profiles of oxygen, nitrate, nitrite, ammonium, phosphate, as well as depth distributions of temperature, salinity, and potential density. Depth distributions for nitrate, nitrite, ammonium, and phosphate were interpolated from the available data using cubic spline and linear fits that preserved the absolute values and the overall trends of the measured points.

The color imagery was processed as a stack.[28] Images that fell within 0.25 m of the target altitude were used to calculate the mean and standard deviation per pixel position. Over the stack of images we assume that the distribution of intensities for any pixel position should be the same regardless of the pixel position. In practice, they are not since illumination tends to drop off toward the edges of the image. To compensate for this effect, at each pixel position, a gain and offset per channel was applied to match a target mean and standard deviation (that of the central pixel). However, images higher than the altitude band will appear darker and shifted toward blue/red given the preferential attenuation of reds with increased range. Images below the altitude band will appear brighter and shifted toward red. To compensate for this effect, an exponential as a function of altitude was robustly fit to the average intensity per channel for each image. Using these empirical attenuation coefficients we were able to express the average intensities at a standard altitude of 3.5 m.

Bathymetric, chemical, and color spatial analyses were performed using the ∼30 m resolution U.S. Coastal Relief Model (CRM) freely available from the NOAA National Geophysical Data Center (www.ngdc.noaa.gov/mgg/coastal/crm). Average image color (AUV *Sentry*) and interpolated chemical depth profiles (CalCofi) were projected onto the corresponding bathymetric depths throughout the SBB to create 2-D and 3-D spatial representations of the data. In addition, the ∼30 m bathymetry was used to perform calculations with volume and surface area components (i.e., nitrogen uptake by sediment and water column denitrification).

Autonomous collection of bacterial communities was conducted in the benthic boundary layer to identify organisms potentially sourced from the sea floor. Collection was performed with the AUV-mounted SUPR sampler, used to filter microbes from seawater at three depths: 574−575 m, 327−357 m, and 90−95 m. Each sample was collected 3.5 m from the sea floor, onto a 0.2 μm poresize filter (142 mm diameter, poly(ether sulfone)). Filtration was concurrent with the photoimaging survey, and samples were frozen at −80 °C immediately following the completion of the survey. Stored DNA was extracted from the filters and sequenced for 16S rRNA amplicons by Illumina MiSeq (300 nucleotide length paired-end reads using the v3 platform) according to the manufacturers specifications.[29] Sequence taxonomies were assigned by aligning processed reads with the SILVA small subunit rRNA database.[30] Closely related and identically classified sequences were pooled into operational taxonomic units (OTUs). OTUs closely related to known biofilm-forming,

DOI: 10.1021/acs.est.6b03584
Environ. Sci. Technol. XXXX, XXX, XXX−XXX

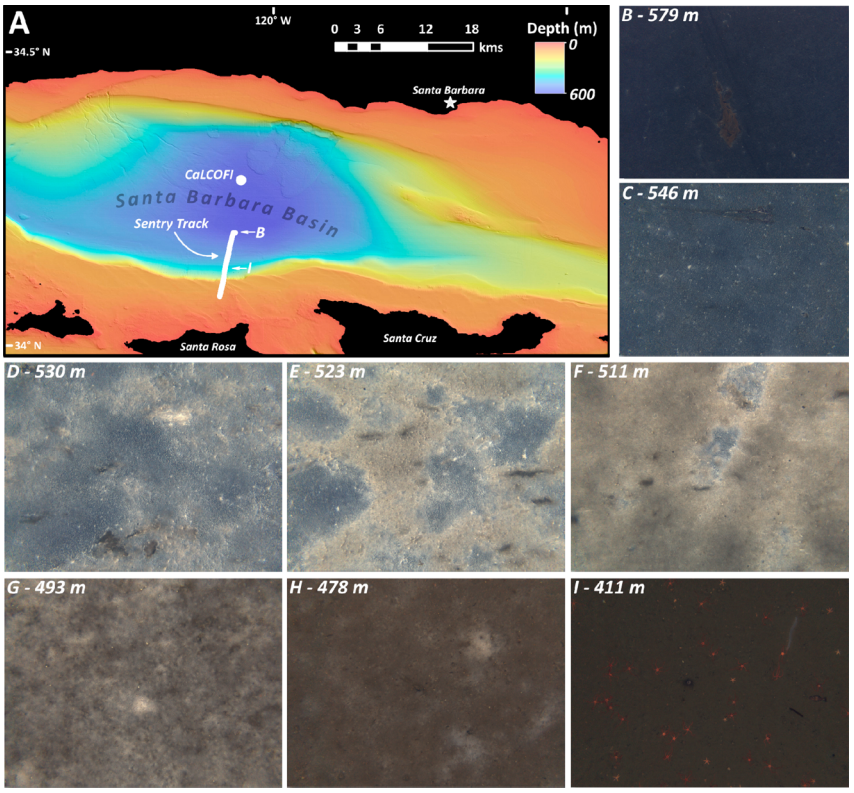

Figure 1. (A) Bathymetry of the Santa Barbara Basin derived from the ~30-m resolution Coastal Relief Model and overlaid with the photoimaging survey track collected by AUV Sentry and the CalCOFI sampling site. (B–I) Color images and their depths collected along the Sentry transect: (B) kelp fall and associated drag marks in the deep basin; C) initiation of spotted mat coverage on otherwise barren seafloor; (D-F) increasing mat coverage culminating in near full contiguity; (G-I) transition from near complete mat coverage to absence of mats and marked presence of abundant macrofauna. Horizontal image scales: B = 2.70 m; C = 2.65 m; D = 2.56 m; E = 2.60 m; F = 2.71 m; G = 2.50 m; H = 2.50 m; I = 2.55 m. Full resolution versions of panels B, F and I are provided in Figure S1.

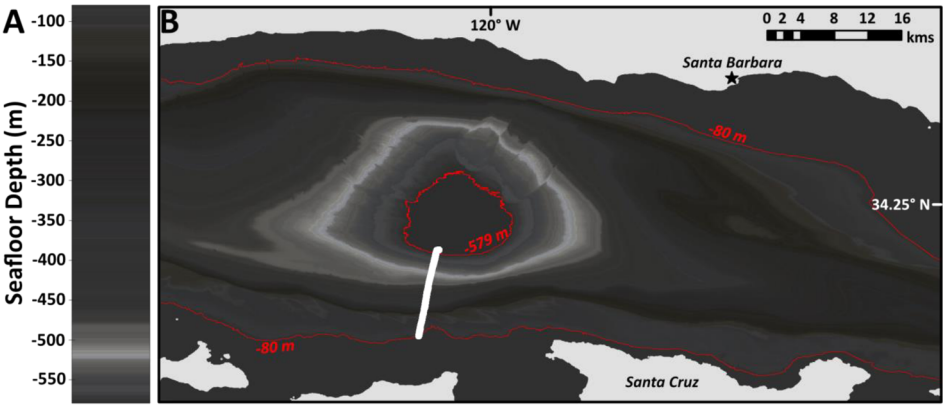

Figure 2. (A) Average sea floor color as a function of depth. The averages were determined from 31,209 color images taken during the AUV *Sentry* survey. (B) Average RGB values projected onto the bathymetry between depths of 80 and 579 m. The red contours indicate the upper and lower depth contours of the survey; coloration <80m and >579m is shown as being constant and matching to the nearest 1m interval for which images are available. The track of the imaging survey is shown as a white line.

nitrate-reducing, sulfur-oxidizing bacterial taxa (NR-SOB), and other putative sulfur-cycling groups, were compared between samples.

RESULTS AND DISCUSSION

An Expansive Community of Mat-Forming Bacteria. The mission plan for this operation included: a photoimaging survey from the deep (579 m), suboxic SBB to the oxygenated continental shelf (80 m), with sufficient image overlap to generate a single contiguous photomosaic image along this redox gradient; collection of bacteria and suspended particulate matter from the benthic boundary layer by filtering large volumes of water in situ during transit; and a high-resolution bathymetric survey from the continental shelf back to the central basin. The photoimaging portion of the AUV *Sentry* operation described here was 12.5 km in length and captured >31 000 stereopaired images of the sea floor, at a target altitude of 3.5 m. The images captured dense faunal assemblages in the oxygenated zone, in contrast to a paucity of fauna in the suboxic

DOI: 10.1021/acs.est.6b03584
Environ. Sci. Technol. XXXX, XXX, XXX–XXX

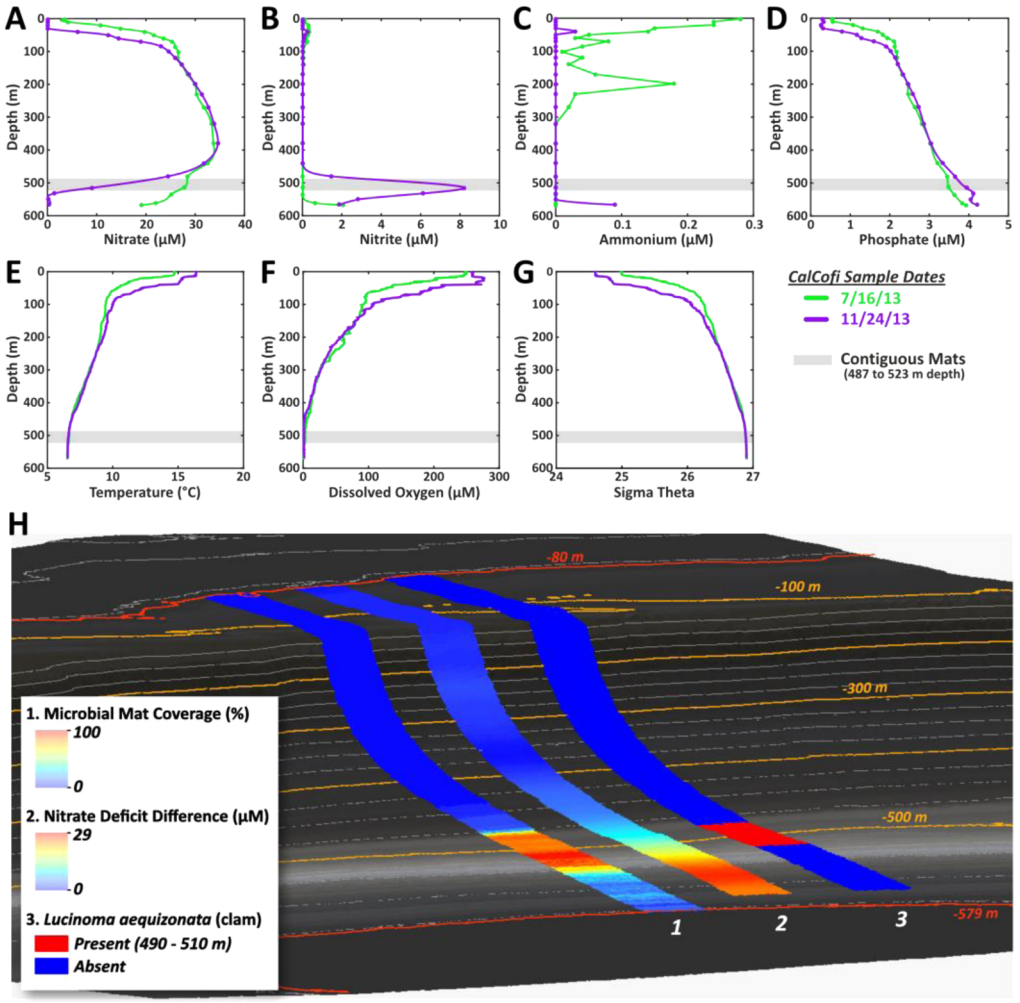

Figure 3. (A–G) Depth distributions from CalCOFI data sets collected July 16, 2013 and November 24, 2013, for (A) Nitrate, (B) Nitrite, (C) Ammonium, (D) Phosphate, (E) Temperature, (F) Dissolved Oxygen, and (G) Sigma Theta. (H) Three data sets overlaid on the bathymetry of the southern margin of the SBB (10x vertical exaggeration) and average seafloor color from the AUV *Sentry* survey (from Figure 2), including the estimated mat coverage (%) along the photo survey transect (strip 1), the difference in nitrate deficit (eq 1) between July and November (strip 2), and the habitat depth range of the endosymbiont-bearing bivalve *Lucinoma aequizonata* (strip 3).[32]

zone. In the deep suboxic water, images captured dark linear features, seemingly from detrital material dragged across the sea floor, as well as kelp falls and mats of filamentous bacteria. Figure 1 displays *Sentry*'s mission track and exemplary images.

Surprisingly, the images from this survey revealed a thick span of bacterial mat 2.3 km in length, within the discrete depth interval of 479–532 m. Based on the images within this interval we estimate that mats residing between 487 and 523 m covered more than 80% of the sea floor and seemingly formed a single interconnected structure. At depths greater than 532 m the distribution of mats was patchy and the abundance decreased with increasing depth. Similarly, the distribution of mats was patchy and decreased between 479 and 450 m, and mats were absent at depths shallower than 450 m. Figure 2A displays the average color of the sea floor as a function of depth, highlighting the zone inhabited by the white-colored, mat-forming bacteria.

The clear association of mat appearance with known redox stratification of the SBB[23,31] water column leads us to predict a similar depth distribution of mat throughout the basin, at the time of the survey—a so-called "bathtub ring". While not explicitly tested through additional surveys, we attempted to visualize this predicted pattern by averaging the altitude-corrected image color in 1 m depth bins and extrapolating the colors as overlay on the bathymetric contours of the SBB (Figure 2). The resulting extrapolation yields a contiguous, annular bacterial mat with a circumference of 106 km (Figure 2B), and an area of 265 km^2, situated between 487 and 523 m water depth. If the extrapolation is accurate, this structure could represent the largest contiguous bacterial growth yet mapped. While this distribution must be treated as a hypothesis, additional support for the vertical stratification of benthic communities at this depth in the SBB comes from reports of the endosymbiont-bearing bivalve *Lucinoma aequizonata* (Figure 3), found in the sediments of the SBB at a narrow range of water depth, 500 ± 10 m.[32]

Do Mat-Forming Bacteria Modulate Regional Nitrogen Biogeochemistry? To assess the biogeochemical context of the observed bacterial mats we looked to bracket our observations with repeat surveys performed by the California Cooperative Oceanic Fisheries Investigations (CalCOFI) program,[33] which typically include the occupation of one station in the central SBB. We found that our survey was well bracketed by these occupations, which occurred on 16 April, 15

DOI: 10.1021/acs.est.6b03584
Environ. Sci. Technol. XXXX, XXX, XXX–XXX

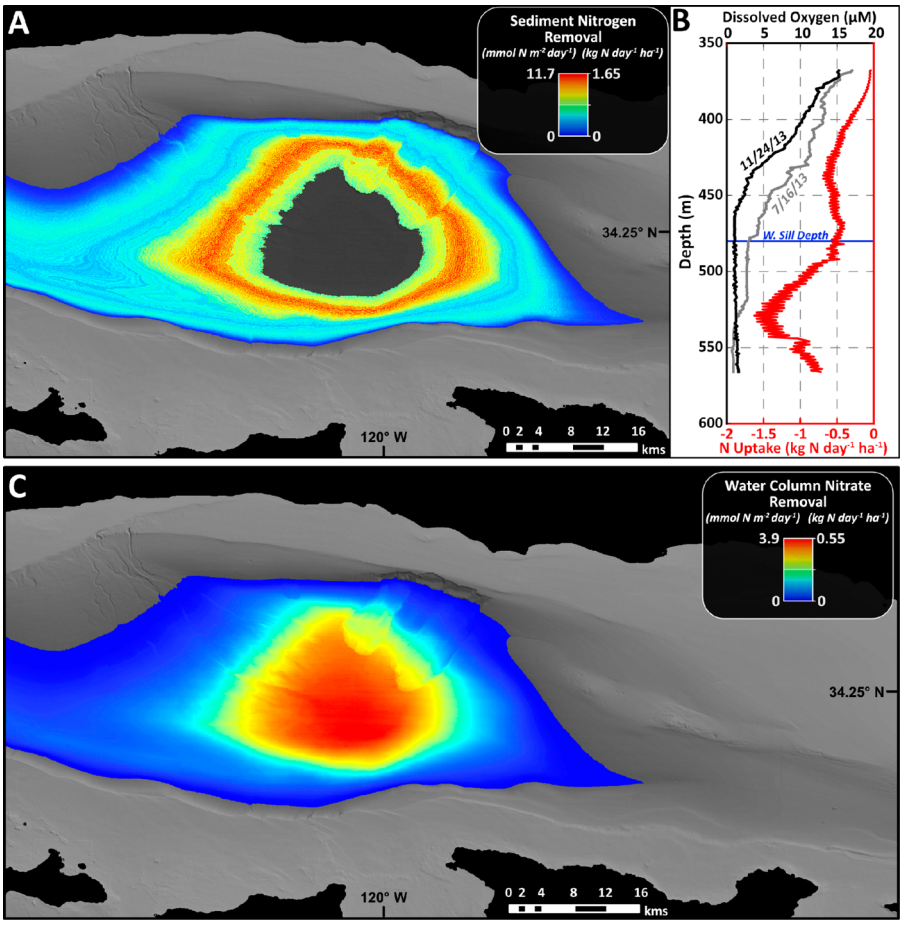

Figure 4. Hypothesized rates of nitrogen removal in the SBB by sedimentary processes and water column denitrification. (A) Areal view of calculated nitrogen uptake rates to the sediment between depths of 368 and 566 m assuming no vertical mixing of the water column and fractional biological nitrate transport to sediment of 75%. (B) Depth profile displaying the calculated nitrogen uptake rate used to populate panel A and CalCOFI dissolved oxygen profiles (expanded from Figure 3F) from July and November. (C) Column-integrated rate of (water column) denitrification assuming 75% fractional loss to sediment.

July, and 24 November of 2013. These time series data indicate that the SBB experienced typical flushing[31,34] in the Spring of 2013 but that conditions in the deep basin were again suboxic by 15 July and through 24 November (Figure 3; Figure S2–S4). In contrast to the minor change in oxygen concentration between 15 July and 24 November (Figure 3F), nitrate concentration decreased dramatically (Figure 3A), clearly defining its importance as the primary terminal oxidant metabolized during this interval. The extent of nitrate loss was calculated from interpolated depth profiles of nitrate, nitrite, ammonium and phosphate (including a correction for preformed phosphate—defined as phosphate present independently of organic matter decomposition that occurred after the water left the sea surface[35]), with the nitrate deficit calculated from the deficiency in bioavailable nitrogen—relative to phosphate,[36] as follows:

$$\text{nitrate deficit} = 16 \times [PO_4^{3-}] - [NO_3^-] - [NO_2^-] - [NH_4^+] \quad (1)$$

Depth distribution of the change in nitrate deficit is displayed in Figure 3H, representing the removal pattern of bioavailable nitrogen from the water between 15 July and through 24 November.

The vertical banding of the bacterial mats in the SBB was observed concurrent with depletion of nitrate within the same depth interval and with the upward expansion of the chemocline (Figure 3A, 3H). While these observations are insufficient to distinguish water column versus sedimentary processes, sediments of the SBB have long-been suspected as the primary nitrate sink[37] and authors of a previous study in the SBB[12] provide evidence that "sedimentary denitrification accounts for more than 75% of the nitrate loss within the suboxic SBB". While we are unable to distinguish nitrate uptake to bacterial mats versus other sedimentary processes, we are able to estimate rates of benthic nitrate uptake (presumably leading to nitrogen loss by annamox/denitrification) and water column denitrification in a spatially resolved manner (Figure 4). We therefore estimated nitrate removal from the change in water column nitrate deficit (i.e., eq 1) between 15 July and 24 November by assuming: a linear decrease over this interval; that 75% of the nitrate deficit was through sedimentary processes;[12] and that nitrate was sourced laterally (i.e., horizontal motion ≫ vertical motion) (Figure 4A). These calculations for sediment nitrate uptake (Figure 4A) and (water) column-integrated denitrification (Figure 4C) provide estimates for loss of fixed nitrogen in this environment: up to 11.7 mmol N d^{-1} m^{-2} (1.65 kg N d^{-1} ha^{-1}) by the mat-coated sediment situated between 479 and 532 m water depth and up to 3.9 mmol N d^{-1}

DOI: 10.1021/acs.est.6b03584
Environ. Sci. Technol. XXXX, XXX, XXX−XXX

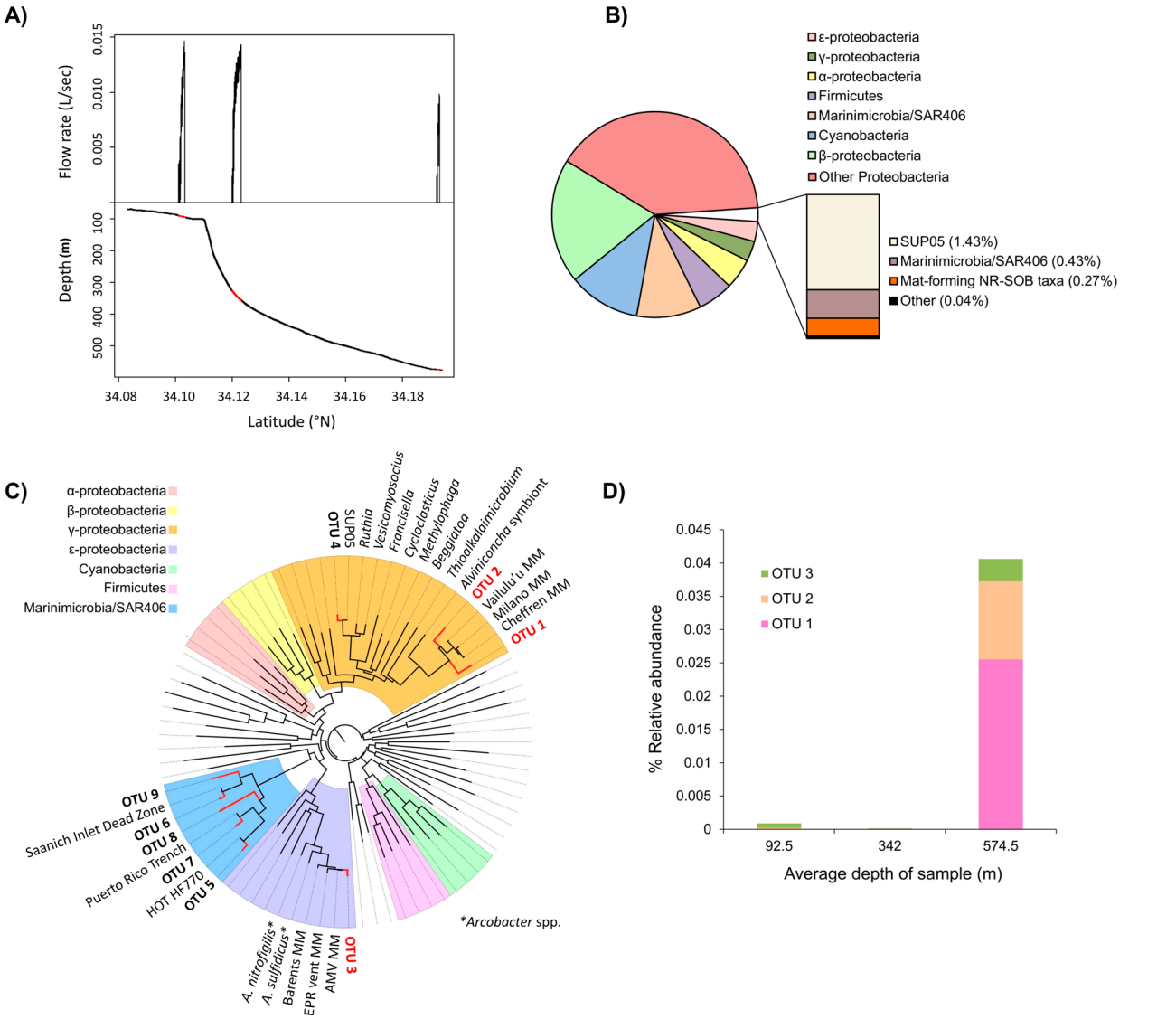

Figure 5. Microbial community composition of the benthic boundary layer as sampled by AUV. (A) Filtration rate, depth, and location along transect. (B) Bacterial community structure of the SBB benthic boundary layer at 574−575m. The call-out bar displays the further breakdown in relative abundances of putative sulfur-oxidizing bacteria. (C) Neighbor-joining tree of sequences from putative SBB sulfur-oxidizing bacteria (red branch tips) within a broader context of bacterial phylogeny (black tips). Branch labels with "MM" refer to environmental microbial mat samples. (D) Depth distribution of sequences closely related (>98%) to either known nitrate-reducing, sulfide-oxidizing bacteria (NR-SOB) or to environmental samples from thiotrophic microbial mats.

m^{-2} (0.55 kg N d^{-1} ha^{-1}) integrated through the full depth of the water column. The calculated values for nitrate uptake to sediment exceed rates of denitrification observed in other environments.[38,39] Based on observations of persistent suboxia, significant nitrate decline, and expansive coverage of microbial mats, and combined with a known capacity for microbial mats to accumulate nitrate and observations that >75% of denitrification in the SBB occurs in the sediment,[12] we suggest that microbial mats are potentially important to nitrogen biogeochemistry in the SBB.

Ecological and Thermodynamic Factors That May Affect Mat-Forming Bacteria. Within the depth range of 487 and 523 m the observed mat-forming bacteria coated the sea floor with implications for their ecology and the biogeochemistry of the underlying sediment. To provide a conceptual framework for their clear success in this environment we developed a working hypothesis of their fitness landscape (Figure S7). By this perspective we explore the qualitative importance of two key factors potentially contributing to the success of the mat community observed here, with relevance to other marine environments.[40] First, by occupying the entire surface of the sediment and even extending into the overlying water the observed bacteria are expected to overcome the diffusion limitation for supply of nitrate into the sediment,[19] which, based on established physiology, could effectively enable them to choke the supply of nitrate into the sediment. Previous studies at the depocenter of SBB have clearly demonstrated hyper-accumulation of nitrate by this mechanism,[25,41] albeit without the spatial context captured by our AUV survey. Second, the heterotrophic microbial communities underlying these thick mats are thus expected to be deprived of nitrate as oxidant, as has been observed for SBB's depocenter,[25,41] limiting metabolism to lower-energy redox couples and fermentation. Abundant sulfate reduction is expected for this

DOI: 10.1021/acs.est.6b03584
Environ. Sci. Technol. XXXX, XXX, XXX−XXX

scenario, which is perhaps self-evident given the quantity of sulfide needed to support the observed density of microbial mat.

In the context of the sulfide supply needed to support the observed 1.6 km-long span of microbial mat, we modeled its thermodynamic ecology, focusing first on the partitioning of Gibbs Free Energy between sulfide-oxidizing bacteria and the underlying sediment-hosted community containing sulfidogenic anaerobes. A simple thermodynamic approach based on balanced metabolisms for model compounds at steady state conditions (Table S1) demonstrates that by this mechanism bacterial mats have the potential to harvest a majority of the Gibbs Free Energy, leaving the minority to be shared among the underlying community of strict anaerobes. This simplified approach provides insight into the uneven resource partitioning in the observed mat-coated ecosystem driven by a combination of redox stratification and the vast physical coating of mats, but is of limited utility insomuch as it ignores dynamic fluxes of substrates and does not account for denitrification, for example, by annamox bacteria. Nonetheless, these calculations support the expectation that significantly more energy is available to nitrate-reducing bacterial mats than to the underlying community of fermentative, syntrophic, methanogenic, methanotrophic and sulfidogenic anaerobes.

While thermodynamic modeling provides some insight into the SBB's observed mat community, limitations of our observational approach leave open an important ecological question. Is the clear success of this mat community purely opportunistic, or do they benefit from positive ecological feedbacks? More specifically, do these mat communities actively promote the dissimilatory sulfate reduction that shunts reducing equivalents from heterotrophic remineralization through their primary substrate, sulfide? The capacity of these mat communities for environmental manipulation leading to the effective subjugation of anaerobic metabolisms could facilitate their success in the SBB, but remains an open question.

Microbial Mats Are Dynamic Features. Microbial mats respond to rapidly changing environmental conditions, as observed in various settings.[10,42,43] The vertical banding of mats we observed in the SBB occurred in the redoxcline, and serves as a snapshot within a time interval of nitrate removal from the water column (Figure 4). However, the SBB experiences regular cycles of oxygen/nitrate rejuvenation followed by stagnation and gradual reestablishment of the vertical redox gradient, from the depocenter upward. These physical dynamics directly impact the redox conditions at the sediment−water interface and are expected to similarly structure the basin-scale dynamics of microbial mat communities. For example, the coverage of microbial mat at the sediment−water interface may be predicted to follow the upward expansion of the redoxcline, bracketed by complete nitrate depletion on the lower bound and oxygenation (leading to faunal activity and biotubation) at the upper bound. Recruitment of mat-forming bacteria to the sediment−water interface can occur from within the sediment via motility, and our observations indicate a further possibility for seeding from the waters of the benthic boundary layer (Figure 5).

The suggestion that mat dynamics could include recruitment from the water column is consistent with the presence of putative chemolithotrophic bacteria in the benthic boundary layer, as sampled by the AUV (Figure 5). Taxa enriched in the deepest waters sampled (Figure 5D) include those within *Thiotrichales* (OTU 1 and OTU 2) and those closely related to *Arcobacter* (OTU 3), each of which includes known mat-forming, chemolithotrophic, sulfide-oxidizing bacteria.[44,45] Other relevant taxa in this sample, including SAR406 and SUP05 (Figure 5B), contain putative sulfur-oxidizing bacteria, though not necessarily mat-associated.[46−49] The presence of potential mat-forming taxa at 0.27% relative abundance in the undisturbed benthic boundary layer of the deep SBB points to the potential for biological exchange of sediment-hosted and planktonic bacterial communities. Furthermore, the capacity to autonomously sample microbial communities in the benthic boundary layer in the deep ocean is noteworthy because common sampling tools are often problematic for this purpose (e.g., rosette sampling typically halts at 5 m altitude for safety purposes and submersibles frequently alter the benthic boundary layer by sediment disturbance).

The research presented here provides a first detailed look at the depth-related distribution of microbial mats for the SBB and suggests a potentially important role for mat-forming bacteria in driving its nitrogen biogeochemistry, with links to sulfur and carbon biogeochemistry. Still, important questions remain about these communities including their cycle of disturbance and renewal driven by flushing events, the importance of ecological feedbacks, the niche partitioning of different bacterial groups, the coupled spatiotemporal dynamics of their activity, and their impacts on the geologic record as retained in the sediment.

■ ASSOCIATED CONTENT

Supporting Information

The Supporting Information is available free of charge on the ACS Publications website at DOI: 10.1021/acs.est.6b03584.

Additional information as noted in the text (PDF)

■ AUTHOR INFORMATION

Corresponding Author

*E-mail: valentine@geol.ucsb.edu.

Present Address

[▽](J.A.B.) University of Texas Rio Grande Valley, School of Earth, Environmental & Marine Sciences, Brownsville, Texas 78520, United States.

Notes

The authors declare no competing financial interest.

■ ACKNOWLEDGMENTS

This research was made possible by grants from the NSF (OCE-0961725, OCE-1046144, OCE-1036843, OCE-1028990 and OCE-1155855), WHOI's Deep Ocean Exploration Institute, NASA ASTEP (NNX09AB76G) and the Gordon and Betty Moore Foundation through Grants GBMF3306 and GBMF2764. We thank K. Tradd, the Captain and Crew of the RV *Atlantis*, as well as the scientific party of the SEEPS 13 Expedition.

■ REFERENCES

(1) Rabalais, N. N.; Díaz, R. J.; Levin, L. A.; Turner, R. E.; Gilbert, D.; Zhang, J. Dynamics and distribution of natural and human-caused hypoxia. *Biogeosciences* **2010**, 7 (2), 585−619.

(2) Cline, J. D.; Richards, F. A. Oxygen deficient conditions and nitrate reduction in the eastern tropical North Pacific Ocean. *Limnol. Oceanogr.* **1972**, *17* (6), 885−900.

DOI: 10.1021/acs.est.6b03584
Environ. Sci. Technol. XXXX, XXX, XXX−XXX

(3) Canfield, D. E.; Jørgensen, B. B.; Fossing, H.; Glud, R.; Gundersen, J.; Ramsing, N. B.; Thamdrup, B.; Hansen, J. W.; Nielsen, L. P.; Hall, P. O. J. Pathways of organic carbon oxidation in three continental margin sediments. *Mar. Geol.* **1993**, *113* (1−2), 27−40.
(4) Kraft, B.; Tegetmeyer, H. E.; Sharma, R.; Klotz, M. G.; Ferdelman, T. G.; Hettich, R. L.; Geelhoed, J. S.; Strous, M. The environmental controls that govern the end product of bacterial nitrate respiration. *Science* **2014**, *345* (6197), 676−679.
(5) Knowles, R. Denitrification. *Microbiol. Rev.* **1982**, *46* (1), 43−70.
(6) Gruber, N.; Sarmiento, J. L. Global patterns of marine nitrogen fixation and denitrification. *Global Biogeochem. Cycles* **1997**, *11* (2), 235−266.
(7) Christensen, J. P.; Murray, J. W.; Devol, A. H.; Codispoti, L. A. Denitrification in continental shelf sediments has major impact on the oceanic nitrogen budget. *Global Biogeochem. Cycles* **1987**, *1* (2), 97−116.
(8) Hulth, S.; Aller, R. C.; Canfield, D. E.; Dalsgaard, T.; Engström, P.; Gilbert, F.; Sundbäck, K.; Thamdrup, B. Nitrogen removal in marine environments: recent findings and future research challenges. *Mar. Chem.* **2005**, *94* (1−4), 125−145.
(9) Gallardo, V. A. Large benthic microbial communities in sulphide biota under Peru−Chile Subsurface Countercurrent. *Nature* **1977**, *268* (5618), 331−332.
(10) Gallardo, V. A.; Espinoza, C. New communities of large filamentous sulfur bacteria in the eastern South Pacific. *Int. Microbiol.* **2007**, *10* (2), 97−102.
(11) Emmer, E.; Thunell, R. C. Nitrogen isotope variations in Santa Barbara Basin sediments: Implications for denitrification in the eastern tropical North Pacific during the last 50,000 years. *Paleoceanography* **2000**, *15* (4), 377−387.
(12) Sigman, D. M.; Robinson, R.; Knapp, A. N.; van Geen, A.; McCorkle, D. C.; Brandes, J. A.; Thunell, R. C. Distinguishing between water column and sedimentary denitrification in the Santa Barbara Basin using the stable isotopes of nitrate. *Geochem., Geophys., Geosyst.* **2003**, *4*, 5.
(13) Larkin, J. M.; Strohl, W. R. Beggiatoa, Thiothrix, and Thioploca. *Annu. Rev. Microbiol.* **1983**, *37*, 341−367.
(14) Høgslund, S.; Revsbech, N. P.; Kuenen, J. G.; Jørgensen, B. B.; Gallardo, V. A.; van de Vossenberg, J.; Nielsen, J. L.; Holmkvist, L.; Arning, E. T.; Nielsen, L. P. Physiology and behaviour of marine Thioploca. *ISME J.* **2009**, *3* (6), 647−657.
(15) McHatton, S. C.; Barry, J. P.; Jannasch, H. J.; Nelson, D. C. High nitrate concentrations in vocuolate, autotrophic marine Beggitoa spp. *Appl. Environ. Micro.* **1996**, *62* (3), 954−958.
(16) Prokopenko, M. G.; Hammond, D. E.; Berelson, W. M.; Bernhard, J. M.; Stott, L.; Douglas, R. Nitrogen cycling in the sediments of Santa Barbara basin and Eastern Subtropical North Pacific: Nitrogen isotopes, diagenesis and possible chemosymbiosis between two lithotrophs (Thioploca and Anammox) - "riding on a glider. *Earth Planet. Sci. Lett.* **2006**, *242* (1−2), 186−204.
(17) Prokopenko, M. G.; Hirst, M. B.; De Brabandere, L.; Lawrence, D. J. P.; Berelson, W. M.; Granger, J.; Chang, B. X.; Dawson, S.; Crane, E. J.; Chong, L.; et al. Nitrogen losses in anoxic marine sediments driven by Thioploca-anammox bacterial consortia. *Nature* **2013**, *500* (7461), 194−198.
(18) Mußmann, M.; Hu, F. Z.; Richter, M.; de Beer, D.; Preisler, A.; Jørgensen, B. B.; Huntemann, M.; Glöckner, F. O.; Amann, R.; Koopman, W. J. H.; et al. Insights into the genome of large sulfur bacteria revealed by analysis of single filaments. *PLoS Biol.* **2007**, *5* (9), e230.
(19) Zopfi, J.; Nielsen, L. P. Ecology of *Thioploca* spp.: Nitrate and sulfur storage in relation to chemical microgradients and influence of *Thioploca* spp. on the sedimentary nitrogen cycle. *Appl. Environ. Micro.* **2001**, *67* (12), 5530−5537.
(20) Soutar, A.; Crill, P. A. Sedimentation and climatic patterns in the Santa Barbara Basin during the 19th and 20th centuries. *Geol. Soc. Am. Bull.* **1977**, *88*, 1161−1172.
(21) Bernhard, J. M.; Visscher, P. T.; Bowser, S. S. Submillimeter life positions of bacteria, protists, and metazoans in laminated sediments of the Santa Barbara Basin. *Limnol. Oceanogr.* **2003**, *48* (2), 813−828.
(22) Bernhard, J. M.; Buck, K. R.; Farmer, M. A.; Bowser, S. S. The Santa Barbara Basin is a symbiosis oasis. *Nature* **2000**, *403* (6765), 77−80.
(23) Sholkovitz, E. Interstitial water chemistry of the Santa Barbara Basin sediments. *Geochim. Cosmochim. Acta* **1973**, *37* (9), 2043−2073.
(24) Li, C.; Sessions, A. L.; Kinnaman, F. S.; Valentine, D. L. Hydrogen-isotopic variability in lipids from Santa Barbara Basin sediments. *Geochim. Cosmochim. Acta* **2009**, *73* (16), 4803−4823.
(25) Reimers, C. E.; Ruttenberg, K. C.; Canfield, D. E.; Christiansen, M. B.; Martin, J. B. Porewater pH and authigenic phases formed in the uppermost sediments of the Santa Barbara Basin. *Geochim. Cosmochim. Acta* **1996**, *60* (21), 4037−4057.
(26) Kinsey, J. C.; Yoerger, D. R.; Jakuba, M. V.; Camilli, R.; Fisher, C. R.; German, C. R. Assessing the Deepwater Horizon oil spill with the sentry autonomous underwater vehicle. In *2011 IEEE/RSJ International Conference on Intelligent Robots and Systems*; IEEE, 2011; pp 261−267.
(27) Breier, J. A.; Sheik, C. S.; Gomez-Ibanez, D.; Sayre-McCord, R. T.; Sanger, R.; Rauch, C.; Coleman, M.; Bennett, S. A.; Cron, B. R.; Li, M.; et al. A large volume particulate and water multi-sampler with in situ preservation for microbial and biogeochemical studies. *Deep Sea Res., Part I* **2014**, *94*, 195−206.
(28) Johnson-Roberson, M.; Pizarro, O.; Williams, S. B.; Mahon, I. Generation and visualization of large-scale three-dimensional reconstructions from underwater robotic surveys. *J. F. Robot.* **2010**, *27* (1), 21−51.
(29) Illumina. 16S Illumina Metagenomic Protocol http://support.illumina.com/downloads/16s_metagenomic_sequencing_library_preparation.html.
(30) Quast, C.; Pruesse, E.; Yilmaz, P.; Gerken, J.; Schweer, T.; Yarza, P.; Peplies, J.; Glöckner, F. O. The SILVA ribosomal RNA gene database project: improved data processing and web-based tools. *Nucleic Acids Res.* **2013**, *41* (Database issue), D590−6.
(31) Sholkovitz, E. R.; Gieskes, J. M. A physical-chemical study of the flushing of the Santa Barbara Basin. *Limnol. Oceanogr.* **1971**, *16* (3), 479−489.
(32) Cary, S.; Vetter, R.; Felbeck, H. Habitat characterization and nutritional strategies of the endosymbiont-bearing bivalve Lucinoma aequizonata. *Mar. Ecol.: Prog. Ser.* **1989**, *55* (October), 31−45.
(33) CalCOFI. California Cooperative Oceanic Fisheries Investigations http://www.calcofi.org/data.html.
(34) Reimers, C. E.; Lange, C. B.; Tabak, M.; Bernhard, J. M. Seasonal spillover and varve formation in the Santa Barbara Basin, California. *Limnol. Oceanogr.* **1990**, *35* (7), 1577−1585.
(35) Redfield, A. C. The processes determining the concentration of oxygen, phosphate and other organic derivatives within the depths of the Atlantic Ocean. *Phys. Oceanogr. Meteorol.* **1942**, *9* (308), 5−21.
(36) Anderson, J. J.; Okubo, A.; Robbins, A. S.; Richards, F. A. A model for nitrate distributions in oceanic oxygen minimum zones. *Deep-Sea Res., Part A* **1982**, *29* (9), 1113−1140.
(37) Liu, K. E. *Geochemistry of Inorganic Nitrogen Compounds in Two Marine Environments: The Santa Barbara Basin and the Ocean off Peru*; University of California: Los Angeles, 1979.
(38) Hofstra, N.; Bouwman, A. F. Denitrification in agricultural soils: Summarizing published data and estimating global annual rates. *Nutr. Cycling Agroecosyst.* **2005**, *72* (3), 267−278.
(39) Barton, L.; McLay, C. D. A.; Schipper, L. A.; Smith, C. T. Annual denitrification rates in agricultural and forest soils: a review. *Aust. J. Soil Res.* **1999**, *37* (6), 1073.
(40) Thamdrup, B.; Canfield, D. E. Pathways of carbon oxidation in continental margin sediments off central Chile. *Limnol. Oceanogr.* **1996**, *41* (8), 1629−1650.
(41) Prokopenko, M. G.; Sigman, D. M.; Berelson, W. M.; Hammond, D. E.; Barnett, B.; Chong, L.; Townsend Small, A. Denitrification in anoxic sediments supported by biological nitrate transport. *Geochim. Cosmochim. Acta* **2011**, *75* (22), 7180−7199.

DOI: 10.1021/acs.est.6b03584
Environ. Sci. Technol. XXXX, XXX, XXX−XXX

(42) Ding, H.; Valentine, D. L. Methanotrophic bacteria occupy benthic microbial mats in shallow marine hydrocarbon seeps, Coal Oil Point, California. *J. Geophys. Res. Biogeosciences* **2008**, *113* (1), 1−11.
(43) Troelsen, H.; Jørgensen, B. B. Seasonal dynamics of elemental sulfur in two coastal sediments. *Estuarine, Coastal Shelf Sci.* **1982**, *15*, 255−266.
(44) Garrity, G.; Bell, J.; Lilburn, T. Thiotrichales ord. nov. *Bergey's Manual of Systematic Bacteriology* **2005**, 131−210.
(45) Wirsen, C. O.; Sievert, S. M.; Cavanaugh, C. M.; Molyneaux, S. J.; Ahmad, A.; Taylor, L. T.; DeLong, E. F.; Taylor, C. D. Characterization of an autotrophic sulfide-oxidizing marine Arcobacter sp. that produces filamentous sulfur. *Appl. Environ. Microbiol.* **2002**, *68* (1), 316−325.
(46) Wright, J. J.; Mewis, K.; Hanson, N. W.; Konwar, K. M.; Maas, K. R.; Hallam, S. J. Genomic properties of Marine Group A bacteria indicate a role in the marine sulfur cycle. *ISME J.* **2014**, *8* (2), 455−468.
(47) Hawley, A. K.; Brewer, H. M.; Norbeck, A. D.; Paša-Tolić, L.; Hallam, S. J. Metaproteomics reveals differential modes of metabolic coupling among ubiquitous oxygen minimum zone microbes. *Proc. Natl. Acad. Sci. U. S. A.* **2014**, *111* (31), 11395−11400.
(48) Glaubitz, S.; Kießlich, K.; Meeske, C.; Labrenz, M.; Jürgens, K. SUP05 dominates the Gammaproteobacterial sulfur oxidizer assemblages in pelagic redoxclines of the central Baltic and Black Seas. *Appl. Environ. Microbiol.* **2013**, *79* (8), 2767−2776.
(49) Marshall, K. T.; Morris, R. M. Isolation of an aerobic sulfur oxidizer from the SUP05/Arctic96BD-19 clade. *ISME J.* **2013**, *7* (2), 452−455.

DOI: 10.1021/acs.est.6b03584
Environ. Sci. Technol. XXXX, XXX, XXX−XXX